https://doi.org/10.2352/lim.2024.5.1.17

SiCAM: Spectral image Color Appearance Model

***Aqsa Hassan*[1,2]*, Giorgio Trumpy*[2]*, Susan Farnand*[1]*, and Mekides Assefa Abebe*[1]**
[1] ***The Munsell Color Science Lab, Rochester Institute of Technology &*** [2] ***The Department of Computer Science, Norwegian University of Science and Technology***

Abstract

In the past, several research studies have highlighted the idea that spectral data produces better tone-accurate images. Inspired by these studies, this paper introduces the spectral image color appearance model titled SiCAM, designed for tone mapping an HDR hyperspectral radiance cube to a three-channel LDR image. It is to be noted that SiCAM is inspired by the iCAM06 image color appearance model, where we adapted the iCAM06 for hyperspectral input by embedding a spectral adaptation transformation, extending the existing chromatic adaptation transform (CAT) method. Additionally, we conducted a psychophysical experiment to evaluate the proposed model and the effectiveness of having spectral data instead of traditional three-channel input, for HDR image rendering. The proposed model is also assessed in comparison to the performance of iCAM06 and the gamma tone mapping approaches. The subjective evaluation indicates that SiCAM either outperformed these methods in terms of both accurate color appearance and pleasantness or at least generated comparable results. This also hints that the spectral information might be able to improve not only the acquisition capabilities but also display rendering. Due to the lack of publicly available HDR spectral datasets, we captured the HDR hyperspectral radiance images of four different HDR scenes which will be made available along with the related source code.

Introduction

High dynamic range (HDR) imaging requires tone-mapping to scale the large range of luminance that exists in real-world scenes so that it can be displayed on a standard dynamic range (SDR) display. Tone mapping attempts to reproduce the original HDR scene appearance including contrast, sharpness, and color while overcoming the output device limitations. Existing tone mapping algorithms have been proposed only for traditional three-channel (i.e., RGB) HDR images [1, 8, 10, 19, 22]. Owing to the fact that having spectral data can produce better color-accurate images, this paper aims to investigate how the perceptual quality and realism in HDR-rendered images are affected by using HDR hyperspectral data instead of traditional three-channel HDR images. Moreover, past research studies have also highlighted that although trichromatic vision serves as the first stage of color vision processing at the retinal level [5, 13], it might be possible that the higher levels of the visual pathway might have some access to spectral data which may complement trichromatic mechanisms. For instance, the idea of spectral adaptation was first introduced by Fairchild [11] which was inspired by this idea of spectral visual processing. In addition, researchers are already investigating different aspects of the spectral imaging chain as highlighted in the following paragraph. Hence foreseeing the future advancements where the whole capture-to-reproduction pipeline works on spectral processing, our research attempts to incorporate spectral data into the traditional trichromatic imaging pipeline, where different existing and future research studies focused on leveraging spectral processing can benefit from it. This work also hints that the spectral information might be able to improve not only the camera capture side but also display rendering. It is well known that having multispectral data can produce better color-accurate images [3, 16], but whether the same thing can be said for tone mapping too or not has not been explored yet.

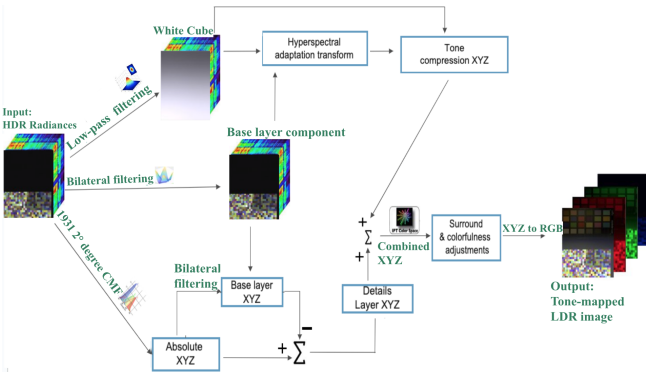

Figure 1. *The diagram illustrates the working pipeline of proposed SiCAM for rendering HDR images.*

In the past, only a few studies have attempted to integrate hyperspectral data to increase the quality and color accuracy of HDR image reconstruction. M. A. Martinez et al. [20] proposed a framework for capturing spectral reflectance through HDR hyperspectral imaging where the authors used three different focus settings and for each focus, three different exposure times were used to obtain the spectral range from 400nm to 1000nm. Lapray et al. [17] also presented an interesting work that combined HDR and spectral imaging by proposing an HDR spectral imaging pipeline for multispectral filter array cameras which was intended to estimate relative multi-spectral radiance of HDR scenes. This has resulted in channel balance correction and noise reduction. A novel hyperspectral visualization approach based on HDR was developed by Ertürk et al. [9] which aimed to retain the high visual quality details while converting hyperspectral images to three-channel color images. Khan, H. A et al. [14] proposed the idea of multispectral constancy by leveraging Spectral Adaptation Transform (SAT), which allowed the acquisition of multispectral images independent of illumination.

Most studies, generally, focus on either three-channel HDR or low dynamic range hyperspectral imaging. Research combining both HDR and hyperspectral information is limited. Chromatic Adaptation transforms (CAT) and perceptual tone mapping for HDR hyperspectral image data have not been well explored. Additionally, finding hyperspectral images with higher luminance ranges was challenging. Only a few datasets are available for three-channel HDR images [10, 21, 28, 29] and hyperspectral images [4, 7] separately.

Our study addresses these limitations by extending CAT

to the hyperspectral domain, and processing and evaluating the effectiveness of hyperspectral HDR radiance data for accurate HDR image rendering. The main contributions of our study are:

- A framework for HDR hyperspectral data acquisition, post-processing, and rendering.
- A new adaptation of the iCAM06 color appearance model, SiCAM, designed for perceptual transformation of HDR hyperspectral radiance cubes to SDR images (Figure 1).
- The Hyperspectral Adaptation Transform (HAT), extending CAT processes into the hyperspectral domain.
- Four HDR hyperspectral radiance images.

Data acquisition and processing

The HySpex VNIR-1800 line scanner was used to capture HDR hyperspectral data, covering a spectral range of 400nm to 1000nm with 186 bands at 3.26nm intervals. The HDR scene included a bright LED backlight with a reflective color checker on one side to create dark regions, and a transmissive (chromogenic film) color target on the other side to create highlights, as shown in Figure 2. A neutral density filter was also added to the top corner of the transmissive color target to create mid-tones. A halogen lamp partially illuminated the reflective color checker to raise the luminance of the dark regions, which the hyperspectral camera struggled to capture at its maximum integration time setting. Only the area within the red borders in Figure 2 was included in our HDR scene, which was set up as a flat scene with low depth due to the camera's limited depth of field. The detailed

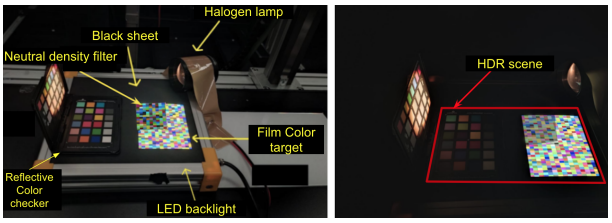

Figure 2. *The HDR scene setup is illustrated on the left side, with room lights turned on for demonstration. Only the area within the red borders is captured with the hyperspectral camera, as shown in the image on the right.*

workflow for HDR hyperspectral data capture and processing is presented in Figure 3. To properly capture the details of our HDR scene, two hyperspectral cubes were captured at the exposure of 20ms and 40ms. These short exposure settings were empirically selected to effectively capture the details residing in the brighter regions of this scene. The third hyperspectral cube was acquired at a longer exposure setting of 440ms to capture details of the darker regions. Additionally, three dark frames were captured with the lens cap in the dark room, at each identical exposure settings (i.e. 20ms, 40ms, and 440ms) to perform the dark current correction. HySpex VNIR-1800 stores the captured data in 16-bit raw digital numbers. Later, these three hyperspectral captures were then converted to absolute radiances and individually stored in 32-bit file float format through the HySpex software package.

According to the characterization, the hyperspectral camera's linearity was valid up to 40,000 digital counts, beyond which data capture became unreliable. To correct this, a look-up table (LUT) based non-linearity correction [26] was applied. This involved storing scaling factors in the LUT, representing the ratio of the 'ideal' response to the measured response. These factors corrected the radiance values for digital counts in the non-linear region, as digital numbers and radiances are directly proportional. The correction was applied to 63,000 digital counts to

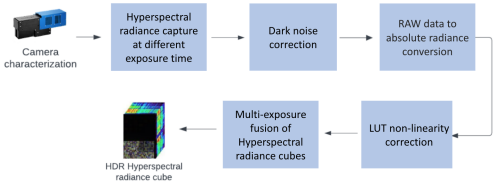

Figure 3. *The workflow for processing hyperspectral data to calculate hyperspectral HDR radiance cube.*

leave some headroom for extremely non-linear data. Finally, the three individual hyperspectral radiance images were fused based on a rectangular-shaped weighting function. The merging with such weighting helps to discard the pixel values affected by dark noise and over saturation at the extreme ends of the camera's sensitivity range. The resultant estimated HDR hyperspectral radiance cube of the HDR scene was stored in a 32-bit float format, with RGBE encoding.

Proposed SiCAM model

To accurately render captured HDR hyperspectral radiance images, we introduce SiCAM, a color appearance model extending the iCAM06 model [15]. SiCAM retains the original perceptual principles while incorporating a hyperspectral radiance processing pipeline and a Hyperspectral Adaptation Transform (HAT) instead of the traditional three-channel CAT. Figure 1 outlines the SiCAM workflow, with newly introduced processing steps discussed in the following subsections:

Bilateral filtering for base layer

The first step in the iCAM06 model is splitting the input image into base and detail layers, reflecting the human vision system's sensitivity to local contrast (detail layer) over global contrast (base layer). As shown in Figure 1, SiCAM uses an HDR hyperspectral radiance cube input instead of a three-channel HDR image, and the goal is to preserve spectral information through most of the initial processing stages. In SiCAM, base layer is obtained by applying the bilateral filter channel-wise on the input image. The bilateral filtering [6, 25] is a non-iterative edge preserving Gaussian smoothing as given by equation 1 where $J_{s_{ch}}$ is the output pixel value at location s_{ch}, f is the function that operates on spatial domain, g is the function which works on pixel intensities, Ω is the kernel window around the central pixel and k_{ch} is the normalizing function to constraint the sum of the weights equal to 1. Both f and g are defined as Gaussian in this equation and M represents the number of channels in the hyperspectral image.

$$J_{s_{ch}} = \frac{1}{k_{ch}(s_{ch})} \sum_{p_{ch} \in \Omega} f(p_{ch} - s_{ch}) g\left(I_{p_{ch}} - I_{S_{ch}}\right) \quad I_{p_{ch}} \qquad (1)$$

$$where; \quad k_{ch}(s_{ch}) = \sum_{p \in \Omega} f(p_{ch} - s_{ch}) g\left(I_{p_{ch}} - I_{S_{ch}}\right)$$

$$and, \quad ch \in \{1, 2, \ldots, M\}$$

In iCAM06, bilateral filtering is applied in the XYZ transformation of the input RGB HDR image. In SiCAM, however, this filter is applied directly to the spectral radiance data for each channel, as shown in Equation 1. We believe bilateral filtering in XYZ space can be represented by filtering the spectral information directly. Tristimulus values are linear combinations of incoming spectral radiances with the CIE's Color Matching Function (CMF) [27], as shown in Equation 2 for X, where r is the spectral radiance and $\bar{x}(\lambda)$ is the CMF.

For uniform surfaces, the bilateral filter acts as a regular Gaussian smoothing filter. In areas with details, it performs edge-preserving smoothing by considering both intensity differences and spatial locations of neighboring pixels. In smoother areas, the bilateral filter weights, k, are determined solely by spatial locations, not intensity values. The tristimulus value X can then be calculated as in Equation 3, demonstrating that applying weight k on X is equivalent to applying it on the spectral radiance r, supporting our approach.

$$X = r(\lambda_1)\bar{x}(\lambda_1) + r(\lambda_2)\bar{x}(\lambda_2) + \ldots + r(\lambda_n)\bar{x}(\lambda_n) \quad (2)$$

$$kX = kr(\lambda_1)\bar{x}(\lambda_1) + kr(\lambda_2)\bar{x}(\lambda_2) + \ldots + kr(\lambda_n)\bar{x}(\lambda_n) \quad (3)$$

For detailed areas, weights are calculated considering both spatial locations and intensity values on edges. Therefore, we apply the bilateral filter's edge-preserving weighting function directly in the spectral domain, as shown in Equation 1. While ideally, edges should be more strongly preserved for wavelengths where the HVS is more sensitive, developing a bilateral filter that incorporates human contrast sensitivity is beyond the scope of this work and a potential future research direction.

The base layer results from the spectral bilateral filter, combined with low-pass filter results, is used for chromatic adaptation. The base layer and the input hyperspectral radiance image are transformed to XYZ tristimulus values to calculate the detail layer and combine it back with the chromatically adapted and tone-mapped base layer, as shown in Figure 1.

Hyperspectral Adaptation Transform (HAT)

In place of the three channels CAT, SiCAM uses HAT. The proposed transform (HAT) as given by equation 4 where J' is a 3x1 matrix of tristimulus values, C is Mx3 CIE 2° CMF matrix, and B is Mx1 matrix of the spectral radiance of single spatial pixel location, M is the total number of channels of radiance cube, and D is the partial adaptation factor of the illumination. We define L'_{diag} as a diagonal matrix given by equation 5, where the diagonal entries consist of $D65(\lambda_m)/W(\lambda_m)$ where m defines the number of wavelength samples in the hyperspectral cube, $D65$ is the CIE D65 illuminant spectrum and the W is the white spectral cube that is calculated by applying low pass filtering on the input spectral radiance cube as depicted in Figure 1.

$$J' = C^T(DL'_{diag}B + (1-D)B) \quad (4)$$

$$L'_{diag} = \begin{bmatrix} \frac{D65(\lambda_1)}{W(\lambda_1)} & 0 & \cdots & 0 \\ 0 & \frac{D65(\lambda_2)}{W(\lambda_2)} & \cdots & 0 \\ \vdots & \vdots & \ddots & \vdots \\ 0 & 0 & \cdots & \frac{D65(\lambda_m)}{W(\lambda_m)} \end{bmatrix} \quad (5)$$

Chromatic adaptation in SiCAM is achieved through the calculation of L'_{diag} using Von Kries scaling, adjusted for scene illumination. Instead of using known scene light source spectra as in Fairchild's method [11], we estimate the source white $W(\lambda)$ by applying low-pass filtering to the input hyperspectral cube. Unlike previous methods applied to uniform-colored patches under uniform illumination, our approach handles complex HDR scenes with non-uniform illumination. Besides adapting to D65 illumination, the HAT converts spectral radiances of each pixel to tristimulus XYZ values. The remaining steps in SiCAM, including tone mapping, follow the same iCAM06 model processings [15].

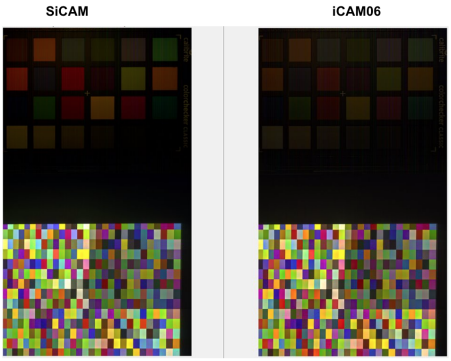

Figure 4. *The comparison of the outputs generated by SiCAM and iCAM06 where the iCAM06's output has an overall slightly yellowish color cast (also see figure 5) while the reflective color checker is hard to be seen.*

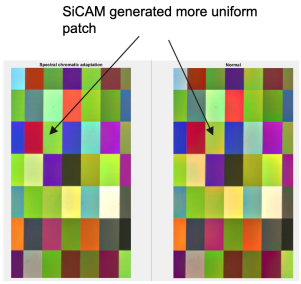

Figure 5. *The figure illustrates the zoomed-in patches of the outputs generated by SiCAM(left-sided) and iCAM06(right-sided) where iCAM06 appears yellowish and less color-accurate (also compare white patches of both outputs).*

SiCAM Results:

Similar to iCAM06, the final output of SiCAM is an 8-bit tone-mapped sRGB image. SiCAM generates sharper and more tone accurate rendering of the HDR hyperspectral images. Figure 4 shows the results, demonstrating better color fidelity with SiCAM. Figure 5 highlights zoomed-in patches where SiCAM's output appears more saturated and visually accurate, with neutral rendering in areas where iCAM06 appears yellowish. These improvements comes from SiCAM's hyperspectral adaptation module, which captures finer spectral details. To further evaluate SiCAM's perceptual accuracy, we conducted an experiment, detailed in the following sections.

Psychophysical experiment

To evaluate SiCAM's performance, we compare its output perceptually with HDR and SDR renderings, as well as the real stimuli setup of the HDR scene. Subjective image quality assessment [18, 23] is the most reliable method for analyzing HDR image quality due to the absence of standardized metrics for evaluating HDR and hyperspectral images. In our experiment, participants rate the quality of HDR and SDR renderings of the HDR hyperspectral image of the scene on both HDR and LDR displays, relative to the provided reference real HDR scene.

Observers

The experiment is conducted with 30 observers, all having normal or corrected vision. Their average age was around 27 years, with most already familiar with image quality assessments and experienced in psychophysical studies. Clear instructions were provided to participants, and a pilot experiment preceded the main one to ensure understanding and accurate rating.

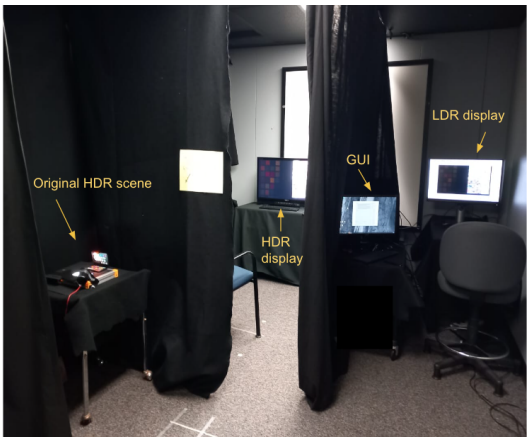

Figure 6. *The experiment was set up in a dark room with three adjoining partitions to avoid interaction for three different types of stimuli during the subjective study which includes an original HDR scene, an HDR image displayed on an HDR monitor, and tone-mapped images which were displayed on an LDR monitor.*

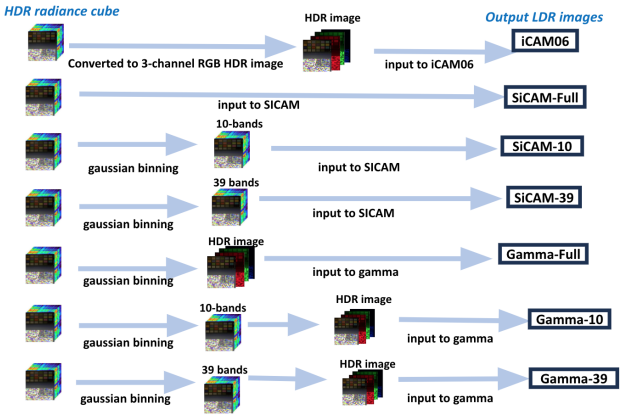

Figure 7. *The figure illustrates that seven tone-mapped images were generated as shown above which were used as test stimuli during the psychophysical experiment.*

Experimental setup

As shown in Figure 6, the experiment was conducted in a dark room with three different partitions containing: a physical HDR scene, an HDR display, and an LDR display. The HDR image was rendered on PVM-X2400 24-inch 4K HDR Sony display, with resolution of 1920-by-1080 pixels and calibrated to REC.2020 PQ mode. Meanwhile, the tone-mapped images were shown to observers on a 24-inch, DELL LDR display with a pixel resolution of 1920-by-1080 and calibrated to sRGB color space. The observers were positioned at a distance of roughly 100cm from the LDR screen and 160cm from the HDR screen. At these distances, each stimulus was subtended approximately 14.25 degrees of visual angle. It is important to note that the white points and luminance ranges of these three types of stimulus (i.e. HDR scene, HDR display, and LDR display) differed significantly. Therefore, participants were required to undergo a minimum adaptation period of 60 seconds for each partition as illustrated in figure 6. The participants were allowed to either complete the experiment in a single sitting based on their memory or they had the option to revisit the original HDR scene at any time during the experiment.

Test stimuli

The HDR hyperspectral radiance cube contained 186 bands spanning 400nm to 1000nm, with a peak luminance exceeding 4000 cd/m^2. However, the visible spectral range of CIE's 1931 2° CMF is from 380nm to 780nm. Consequently, the input cube was clipped to 119 bands within this range. Notably, both the HDR and SDR displays used in the experiment have peak luminances of 1000 cd/m^2 and 230 cd/m^2 respectively, requiring a tone mapping process even for HDR rendering, discussed in the following subsection. In total, seven tone-mapped images of the original HDR hyperspectral radiance capture were utilized, generated using three methods: iCAM06, SiCAM, and gamma tone mapping as illustrated in Figure 7. SiCAM operates on an HDR hyperspectral radiance cube, while iCAM06 and gamma tone mapping require a three-channel HDR image input. Thus, a display-referred HDR rendering pipeline, discussed in the following subsection, is used to convert the original HDR hyperspectral radiance image to a three-channel HDR image input for iCAM06 and gamma approaches. As depicted in Figure 7, more test images were created by reducing spectral bands through Gaussian spectral binning, sampling the 119 bands to 10 and 39 bands chosen empirically. These images from the reduced hyperspectral cube were included to explore the number of bands necessary for better tone-mapped rendering. All test images were displayed against a gray background with luminance equivalent to 20% of the adapting white point of the respective displays.

Display referred HDR rendering pipeline

To convert the hyperspectral radiance capture of the real HDR scene into a three-channel RGB HDR image with a maximum luminance of 1000 cd/m^2, several transformation steps were followed. Initially, the dot product of hyperspectral radiances with CIE's 1931 2° CMF was calculated to estimate three-channel tristimulus values. These were then converted to absolute luminances in cd/m^2 by scaling them with a 683 lm/W constant factor [27]. Our HDR scene's maximum luminance, measured at approximately 4000 cd/m^2 using a CS2000A spectroradiometer, exceeded the HDR display's capability of 1000 cd/m^2. Thus, tone mapping was necessary to compress the scene's luminance within the HDR display's limits, calibrated to REC2020 PQ mode. A gamma of 1.3 was applied to compress the dynamic range of the absolute HDR hyperspectral image to fit within the HDR screen's capabilities. Additionally, we characterized the HDR display to obtain the inverse colorimetric transformation matrix for converting absolute XYZ to linear device dependent RGB values [2]. These converted linear RGB values were then rendered linearly to the PQ mode of the display using the MATLAB Psychtoolbox REC2020 and perceptual quantizer (PQ) encoding-based rendering module [12].

Procedure

In this experiment, three stimuli were used: the original HDR scene, an HDR image displayed on the HDR monitor screen (rendered as described above), and seven tone-mapped LDR images shown on the SDR monitor screen. The experiment assessed both observer preference (pleasantness) and color fidelity (faithful reproduction of original HDR scene colors) of the rendered images. Observers rated each of the seven test SDR images on a scale of 0 to 100, with 100 indicating excellent reproduction and 0 indicating the worst. These images were displayed sequentially, with observers comparing each with the physical HDR scene as a reference. Additionally, observers compared the HDR image rendered on an HDR display with the physical HDR scene, evaluating overall contrast, colorfulness, sharpness, and

Source	DF	SS	MS	F-Stat	P-Value
Between Groups(CA)	6	20954	3492.35	5.67	0.00002
Within Groups(CA)	161	99130.80	515.71		
Between Groups(CP)	63.16	19.349	3.869	13.338	0.0000
Within Groups(CP)	61.28	23.055	4.611		

Table 1. ANOVA for Color Appearance(CA) and Color Pleasantness(CP) Rating Scores.

naturalness.

Experimental results

Figures 8 and 9 show the observers' ratings of color fidelity and pleasantness, while Figure 10 represents ratings for individual attributes of HDR rendering on the HDR display. For color

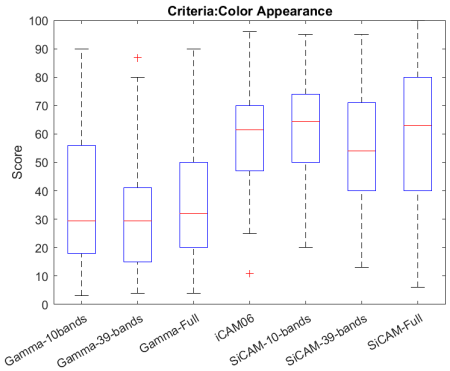

Figure 8. *Subjective scores for color appearance.*

fidelity (Figure 8), observers preferred SiCAM over iCAM06 and gamma tone mapping. The box plot shows ratings for how accurately each method reproduced the physical HDR scene, with the original HDR scene as the reference. SiCAM consistently outperformed the other methods, with gamma TMO receiving the lowest scores. iCAM06 mostly showed comparable performance to SiCAM. Interestingly, SiCAM with 39 bands scored lower than SiCAM with 10 bands and the full spectrum, possibly due to the band selection method, suggesting room for optimization in future research. For pleasantness (Figure 9), both iCAM06 and SiCAM produced similar results, while gamma TMO again scored significantly lower. The comparable performance of iCAM06 with SiCAM is probably due to the fact that the yellowish color cast and nonuniform patch renderings in iCAM06's output (Figure 5) were likely less noticeable to the observers since images were shown to them one at a time without any side-by-side comparison.

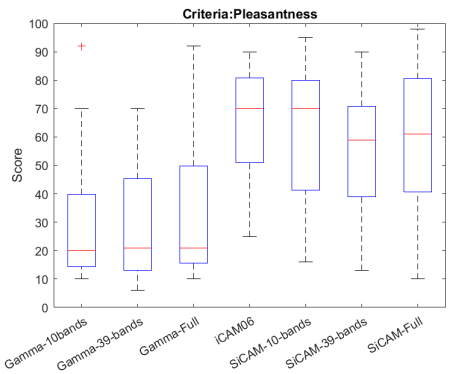

Figure 9. *Subjective scores for pleasantness*

To assess the variability in the observers' ratings, we conducted an ANOVA analysis [24]. The results, summarized in Table 1, show significant differences in both color appearance and pleasantness ratings, with F-stat values and very low p-values (0.00002 for color appearance and 0.0000 for pleasantness). These results, along with the box plots in Figures 8 and 9, indicate a significant difference between the scores for SDR images generated using gamma tone mapping and SiCAM. However, the difference between iCAM06 and SiCAM scores, particularly for pleasantness, is less noticeable.

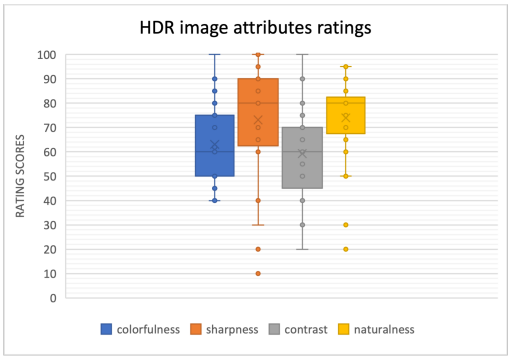

Figure 10. *The rating scores revealed that the sharpness received higher ratings compared to other attributes, while ratings for naturalness varied between 65% and 75%. Colorfulness was slightly better rated than image contrast as depicted from the given plot.*

In addition, the rating scores for the individual attributes of the HDR rendering on HDR display are provided in Figure 10. From the evaluated attributes, image sharpness was given the highest rating, while the rating scores for naturalness varied between 65% to 75%. Furthermore, colorfulness obtained a slightly higher rating, compared to image contrast. Generally, it can be inferred that the overall perceived quality of the HDR image was quite close to that of the physical HDR scene.

Conclusion:

In this study, we investigated how the perceptual quality and realism in HDR-rendered images are affected by using HDR hyperspectral capture of an HDR scene instead of traditional three-channel HDR imaging. We proposed the spectral image color appearance model, SiCAM, designed to perceptually render an HDR hyperspectral radiance images. Although SiCAM is inspired by the latest iCAM06 HDR image rendering model, it significantly extended it to use hyperspectral data and Hyperspectral Adaptation Transform(HAT). The experimental perceptual evaluation results as well as our observations suggest that the proposed SiCAM model generated better or at least comparable results with iCAM06. SiCAM significantly outperformed the conventional gamma based tone mapping rendering approaches. The performance of SiCAM model can be further improved by incorporating more optimal band selection method, perceptual bilateral filtering, and other adjustments such as color saturation compensation and better tone mapping function. Hyperspectral data alone isn't enough for better HDR rendering; an efficient and perceptually accurate processing model is equally important. We also hope the four HDR hyperspectral images we will make openly available will benefit the HDR and hyperspectral imaging community.

References

[1] Francesco Banterle, Alessandro Artusi, Kurt Debattista, and Alan Chalmers. *Advanced high dynamic range imaging*. CRC press, 2017.

[2] Roy S Berns. Methods for characterizing crt displays. *Displays*, 16(4):173–182, 1996.

[3] Roy S Berns. Color-accurate image archives using spectral imaging. *Scientific Examination of Art: Modern Techniques in Conservation and Analysis*, 12:105–119, 2005.

[4] Sol Fernández Carvelo, Miguel Ángel Martínez Domingo, Eva M Valero, and Javier Hernández Andrés. Dehazing in hyperspectral images: the granhhada database. *Scientific Reports*, 13(1):19760, 2023.

[5] Innes C. Cuthill. The biology of color. In *Science*, volume 357,6350, page 0221. New York, N.Y.

[6] Frédo Durand and Julie Dorsey. Fast bilateral filtering for the display of high-dynamic-range images. In *Proceedings of the 29th annual conference on Computer graphics and interactive techniques*, pages 257–266, 2002.

[7] Jia Eckhard, Timo Eckhard, Eva M Valero, Juan Luis Nieves, and Estibaliz Garrote Contreras. Outdoor scene reflectance measurements using a bragg-grating-based hyperspectral imager. *Applied Optics*, 54(13):D15–D24, 2015.

[8] Gabriel Eilertsen, Rafal Konrad Mantiuk, and Jonas Unger. A comparative review of tone-mapping algorithms for high dynamic range video. In *Computer graphics forum*, volume 36, pages 565–592. Wiley Online Library, 2017.

[9] Sarp Ertürk, Seçil Süer, and Hatice Koç. A high-dynamic-range-based approach for the display of hyperspectral images. *IEEE Geoscience and Remote Sensing Letters*, 11(11):2001–2004, 2014.

[10] Mark D Fairchild. The hdr photographic survey. In *Color and imaging conference*, volume 15, pages 233–238. Society of Imaging Science and Technology, 2007.

[11] Mark D. Fairchild. Spectral adaptation. color research and application: Endorsed by inter-society color council, the colour group (great britain), canadian society for color, color science association of japan, dutch society for the study of color, the swedish colour centre foundation. *Colour Society of Australia, Centre Français de la Couleur*, 32(2):100–112, 2007.

[12] International Telecommunication Union. Recommendation ITU-R BT.2100-2. ITU-R Recommendation BT.2100-2, ITU-R, 2018.

[13] A. Kelber. Colour in the eye of the beholder: receptor sensitivities and neural circuits underlying colour opponency and colour perception. *Current opinion in neurobiology*, 41:106–112.

[14] Haris Ahmad Khan, Jean Baptiste Thomas, and Jon Yngve Hardeberg. Multispectral constancy based on spectral adaptation transform. In *Image Analysis: 20th Scandinavian Conference, SCIA 2017*, Tromsø, Norway, June 12–14, 2017. Springer International Publishing.

[15] Jiangtao Kuang, Garrett M. Johnson, and Mark D. Fairchild. icam06: A refined image appearance model for hdr image rendering. *Journal of Visual Communication and Image Representation*, 18(5):406–414, 2007. Special issue on High Dynamic Range Imaging.

[16] Olivia Kuzio and Susan Farnand. Color accuracy-guided data reduction for practical led-based multispectral imaging. In *Archiving Conference*, volume 18, pages 65–70. Society for Imaging Science and Technology, 2021.

[17] Pierre-Jean Lapray, Jean-Baptiste Thomas, and Pierre Gouton. High dynamic range spectral imaging pipeline for multispectral filter array cameras. *Sensors*, 17(6):1281, 2017.

[18] Rafał K Mantiuk, Anna Tomaszewska, and Radosław Mantiuk. Comparison of four subjective methods for image quality assessment. In *Computer graphics forum*, volume 31, pages 2478–2491. Wiley Online Library, 2012.

[19] Rafał Mantiuk, Karol Myszkowski, and Hans-Peter Seidel. High dynamic range imaging. 2015.

[20] Miguel Á Martínez, Eva M Valero, Juan L Nieves, Rosario Blanc, Eloísa Manzano, and José L Vílchez. Multifocus hdr vis/nir hyperspectral imaging and its application to works of art. *Optics Express*, 27(8):11323–11338, 2019.

[21] Manish Narwaria, Matthieu Perreira Da Silva, Patrick Le Callet, and Romuald Pepion. Tone mapping-based high-dynamic-range image compression: study of optimization criterion and perceptual quality. *Optical Engineering*, 52(10):102008–102008, 2013.

[22] Erik Reinhard, Wolfgang Heidrich, Paul Debevec, Sumanta Pattanaik, Greg Ward, and Karol Myszkowski. *High dynamic range imaging: acquisition, display, and image-based lighting*. Morgan Kaufmann, 2010.

[23] David M Rouse, Romuald Pépion, Patrick Le Callet, and Sheila S Hemami. Tradeoffs in subjective testing methods for image and video quality assessment. In *Human Vision and Electronic Imaging XV*, volume 7527, pages 108–118. SPIE, 2010.

[24] Lars St, Svante Wold, et al. Analysis of variance (anova). *Chemometrics and intelligent laboratory systems*, 6(4):259–272, 1989.

[25] Carlo Tomasi and Roberto Manduchi. Bilateral filtering for gray and color images. In *Sixth international conference on computer vision (IEEE Cat. No. 98CH36271)*, pages 839–846. IEEE, 1998.

[26] Giorgio Trumpy, Casper Find Andersen, Ivar Farup, and Omar Elezabi. Mapping quantitative observer metamerism of displays. *Journal of Imaging*, 9(10):227.

[27] Günther Wyszecki and Walter Stanley Stiles. *Color science: concepts and methods, quantitative data and formulae*, volume 40. John wiley & sons, 2000.

[28] Feng Xiao, Jeffrey M DiCarlo, Peter B Catrysse, and Brian A Wandell. High dynamic range imaging of natural scenes. In *Color and imaging conference*, volume 10, pages 337–342. Society of Imaging Science and Technology, 2002.

[29] Emin Zerman, Giuseppe Valenzise, and Frederic Dufaux. An extensive performance evaluation of full-reference hdr image quality metrics. *Quality and User Experience*, 2:1–16, 2017.